Incorporation of Pacific SSTs in a Time Series Model toward a Longer-Term Forecast for the Great Salt Lake Elevation

ROBERT R. GILLIES

Utah Climate Center and Department of Plants, Soils, and Climate, Utah State University, Logan, Utah

OI-YU CHUNG

Utah Climate Center, Utah State University, Logan, Utah

SHIH-YU WANG

Utah Climate Center and Department of Plants, Soils, and Climate, Utah State University, Logan, Utah

PIOTR KOKOSZKA

Department of Mathematics and Statistics, Utah State University, Logan, Utah

(Manuscript received 23 August 2010, in final form 19 November 2010)

ABSTRACT

A recent study identified a pronounced lagged relationship between the Great Salt Lake's (GSL) elevation and the central tropical Pacific sea surface temperatures (SST) at the 10–15-year time scale. Using this relationship, a principal component analysis of historical time series of SST and local precipitation (P) was used in the construction of a lagged regression model to predict first the GSL elevation tendency and, from there, the GSL elevation. The combined principal component–lagged regression model was able to replicate and forecast turnarounds in the GSL elevation—that is, where prolonged increasing trends were followed by persistent decreases and vice versa. The coupling of the two time series is somewhat different from previous nonparametric, nonlinear time series methods developed for shorter-term (1–2 year) forecasts of the GSL volume. Moreover, by not accounting for interannual variability in the model, a forecast out to 6 years was feasible and was shown to intersect the 2009 and 2010 observations of the GSL elevation.

1. Introduction

The elevation of the Great Salt Lake (GSL), Utah, reflects variability on the order of periodic, quasi-periodic, and aperiodic time scales. Such features have challenged numerous attempts to forecast GSL volume variations; for example, by traditional Box–Jenkins methods (James et al. 1984), nonparametric forecasting (Abarbanel and Lall 1996; Lall et al. 1996; Sangoyomi et al. 1996), singular spectral analysis (Moon and Lall 1996), and locally weighted polynomial regression (Lall et al. 2006). Furthermore, based upon the fact that surface hydrologic systems are ultimately forced by the atmospheric circulations, Moon and Lall (1996) and Moon et al. (2008) have included such indices as the monthly Southern Oscillation index (SOI) and the Pacific–North America (PNA) index as predictor variables. Such a combination has resulted in a noticeable improvement in short-term (1–2 year) forecasts for the GSL volume.

In other work, Wang et al. (2010b) discerned that the GSL elevation is highly coherent with, yet opposite to, sea surface temperature (SST) variations in the equatorial Pacific within the 10–15-yr time scale; known as the Pacific quasi-decadal oscillation (QDO) (e.g., White and Liu 2008; Meehl et al. 2009; Wang et al. 2010a). The coherence exists because a trans-Pacific teleconnection wave train develops during the alternating periods between the extreme warm and cool phases of the Pacific QDO and modulates the atmospheric circulations over the Gulf of Alaska; these in turn affect the synoptic patterns and thus the precipitation over the GSL watershed. The

Corresponding author address: Dr. Robert R. Gillies, Utah Climate Center, Utah State University, 4825 Old Main Hill, Logan, UT 84322-4825.
E-mail: Robert.Gillies@usu.edu

DOI: 10.1175/2010JHM1352.1

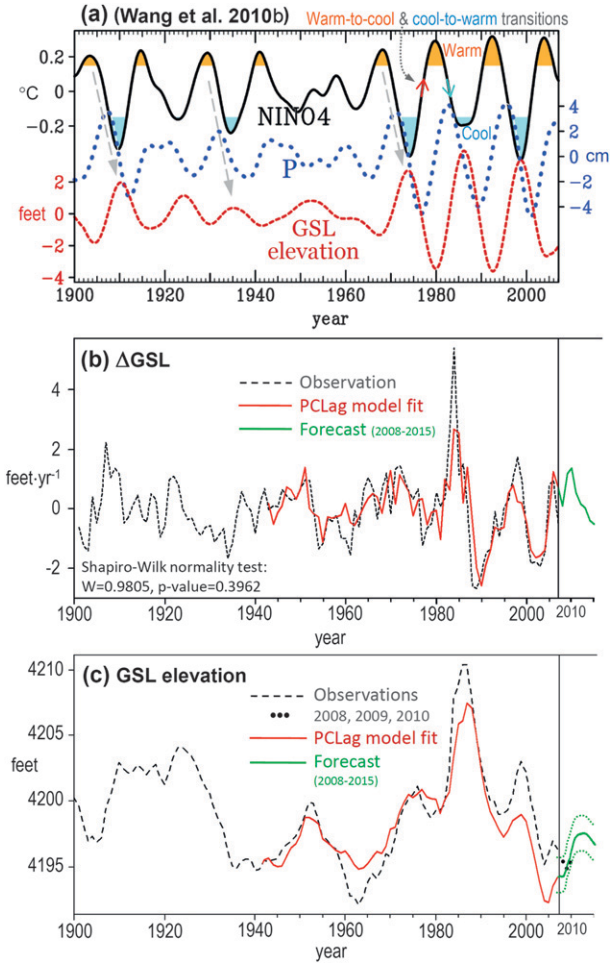

FIG. 1. (a) Adopted from Wang et al. (2010b): 10–15-yr band-passed ΔSST(Niño-4) (black curve; domain 5°N–5°S, 160°E–150°W), precipitation in the GSL watershed (blue dotted curve), and the GSL elevation (red dashed curve). The GSL elevation lags the precipitation by 3 yr, while the precipitation lags the Pacific QDO by another 3 yr. (b) Annual GSL elevation tendency (ΔGSL; black dashed curve) superimposed with the PCLag model fit (red line) and forecast (green line). (c) As in (b), but for the annual GSL elevation; the forecast includes the 95% confidence interval (green dotted curves). Observations of 2008–10 are presented as black dots.

result of these processes is manifest in the precipitation maxima–minima being reached 3 yr (on average) after the extreme phases of the Pacific QDO. It then takes another 3 yr for the GSL to fully integrate such precipitation changes, leading to an overall 6-yr lag between the extremes of the GSL elevation and the Pacific QDO. The entire process is illustrated in Fig. 1a. Given such circumstances, forecasting the GSL elevation out to 6 yr in advance becomes a possibility.

Inspired by the aforementioned linkage between the GSL elevation and the Pacific QDO, this paper investigates the possibility of a longer-term (≥6 yr) forecast of the GSL elevation by utilizing both SST and precipitation time series as predictor variables. Following Wang et al. (2010b), we utilized the Kaplan Extended SST (Kaplan et al. 1998) and the National Weather Service Cooperative Observer Program (COOP) station precipitation (denoted as *P*) for the period of 1900–2007. The COOP station records were provided by the Utah Climate Center (http://climate.usurf.usu.edu/reports/dynamic.php); only the active COOP stations within the GSL watershed were selected for the precipitation analysis (see Wang et al. 2010b for geographical domain and station information). The structure of the paper is as follows: rationale for the proposed models is discussed in section 2, the models are discussed and evaluated in section 3, and conclusions as to the effectiveness of the prediction are given in section 4.

2. Rationale

The water budget equation for a closed-basin lake indicates that any lake volume change is balanced by precipitation, runoff, and evaporation (Shanahan et al. 2007). As a result, any GSL volume change tends to be highly coherent with the precipitation, especially at low-frequency spectrums (Lall and Mann 1995). Thus, it was decided to select the GSL elevation tendency (ΔGSL), rather than the GSL volume, to forecast and reconstruct the GSL elevation. Given our aim toward a longer-term forecast, the seasonal cycle of the GSL elevation, which is on the order of 2 feet, is not of immediate concern. Therefore, the analysis that follows focuses on the annual mean; that is, the ΔGSL was defined as the difference of GSL(t) − GSL(t − 1), where t is the calendar year. Variables SST and P were annual means throughout the water year (August–July) and the calendar year, respectively. The advantage of the described method is twofold: 1) the ΔGSL time series becomes more stationary because of differencing, and 2) ΔGSL is reflective of the GSL's hydrologic forcing, which, as previously noted, directly responds to the Pacific forcings of climate. As shown in Figs. 1b,c (dashed lines), the ΔGSL time series exhibits substantially better stationarity than the GSL elevation, despite a discernible quasi-decadal variability.

3. Models—Construction and evaluation

a. Precipitation-lagged (PLag) regression model

A spectral coherence analysis of ΔGSL and P (Fig. 2a) discloses significant coherence in the frequency bands of 0.13 and 0.06, ~(8 and 17 yr), as was noted in Lall and Mann (1995). Second, an interannual frequency centered at 0.4 appears, which reflects the known influence of El Niño–Southern Oscillation (ENSO) in this region.

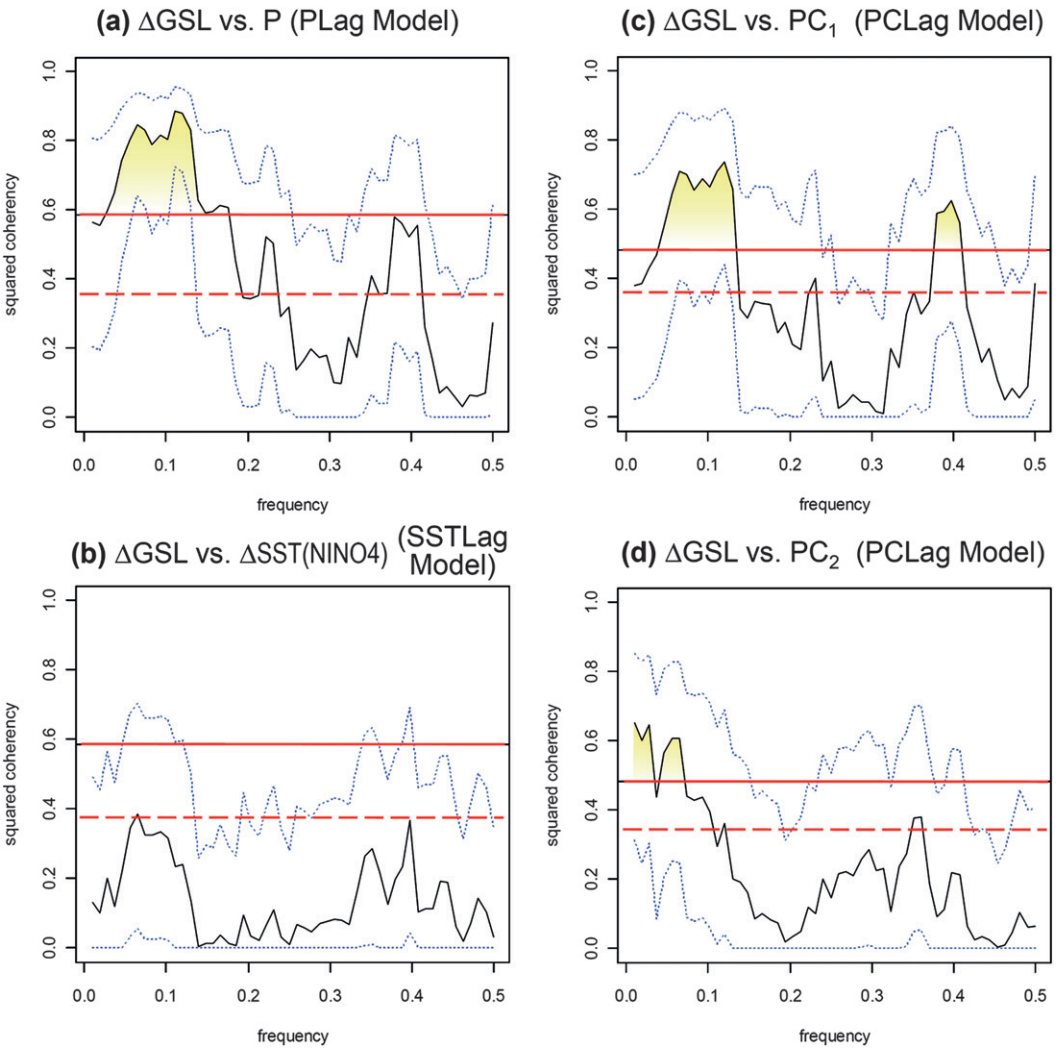

FIG. 2. Spectral coherence between ΔGSL and (a) P, (b) ΔSST(Niño-4), (c) PC_1, and (d) PC_2. Blue dotted curves indicate the 95% confidence interval. Red solid (dashed) line is the rejection criteria at the confidence level of 0.01 (0.05). Significant spectral coherences are shaded in light yellow.

Third and conversely, as is revealed in Fig. 2b, the coherence between the ΔGSL and the SST anomalies in the Niño-4 region [5°N–5°S, 160°E–150°W; ΔSST(NINO4)] is not significant at all. Therefore, based upon the significant coherence between ΔGSL and P, we applied a lagged regression model to relate the two variables. The impulse response function (Shumway and Stoffer 2006) was used to check the initial significant lags. The final lags were chosen through trials based upon the following considerations: 1) the spectral coherence mentioned already, 2) the objective of a longer-term forecast, 3) the multiplied and adjusted model coefficient of determination R^2 and 4) whether the residuals are approximately independent (i.e., form white noise) and are normally distributed. The PLag regression model of choice was

$$\begin{aligned}\Delta\mathrm{GSL} = {} & 0.619\Delta\mathrm{GSL}(t-1) - 0.411P(t-8) \\ & + 0.386P(t-11) - 0.399P(t-17) \\ & + 0.425P(t-42). \end{aligned} \quad (1)$$

Here, all the coefficient betas exceed the 0.05 significance level. Other significant coefficient betas for a shorter lag (<6 yr) were neglected because of the longer-term forecasting purpose. The multiplied and adjusted R^2 of this model was 0.51 and 0.47, respectively. The autocorrelation function (not shown) is within the bound $(-2/\sqrt{n}, 2/\sqrt{n})$, where n is the length of the residuals, meaning that the residuals of the model form approximate white noise. The P value of the Shapiro–Wilk normality test on the residuals was 0.25, suggesting that

TABLE 1. The RMSE between fitted and observed values.

Period	1900–2007	
	ΔGSL (ft)	GSL (ft)
PLag model	0.904	1.206
SSTLag model	1.178	1.564
PCLag model	0.859	1.487

the model captures the data well as the residuals are independently (normal) distributed.

The GSL elevation was then reconstructed by integrating the modeled–forecasted ΔGSL. Because of the maximum lag $t - 42$ in Eq. (1), model fitting and integration are only applicable from 1943 onward (the cause of this 42-yr lag will be discussed later). The root mean square error (RMSE) between the fitted ΔGSL and the observed ΔGSL was 0.904 feet (ft, where 1 ft = 0.305 m; Table 1). The RMSE between the fitted and the observed GSL elevation was 1.21 ft; this is less than the GSL elevation's average seasonal variability.

b. ΔSST(Niño-4)-lagged (SSTLag) regression model

For the sake of completeness, we also constructed an SSTLag regression model, following the same approach as for the PLag model. The best SSTLag model features the same lags as the PLag model, though the coefficient betas did not exceed the 0.05 significance level. However, its large RMSE indicates that the SSTLag model is not superior to the PLag model (Table 1); this was expected given the spectral coherence analysis outlined in Fig. 2b.

c. Principal component-lagged (PCLag) regression model

Given the lagged relationships depicted in Fig. 1a, we were inquisitive about whether a model that incorporates *P* with ΔSST(Niño-4) would result in a better forecast of the GSL elevation than a model with *P* alone. To investigate this, we first undertook a principal component (PC) analysis of the two variables for the 1900–2007 period, which yielded

$$\mathrm{PC}_1 = 0.498 \times \Delta\mathrm{SST(NINO4)} + 0.867 \times P, \quad \text{and} \tag{2a}$$

$$\mathrm{PC}_2 = 0.867 \times \Delta\mathrm{SST(NINO4)} - 0.498 \times P. \tag{2b}$$

Here PC_1 represents a weighted average of ΔSST(NINO4) and *P*, while PC_2 depicts a weighted contrast of the two variables. Figure 3 shows that the projection time series of PC_1 and PC_2 preserve the decadal-scale variability yet appear more stable when compared to the ΔGSL (Fig. 1b). It is noteworthy that rises in ΔGSL usually coincide with a rise in PC_1, while declines in ΔGSL usually follow a decline in PC_2.

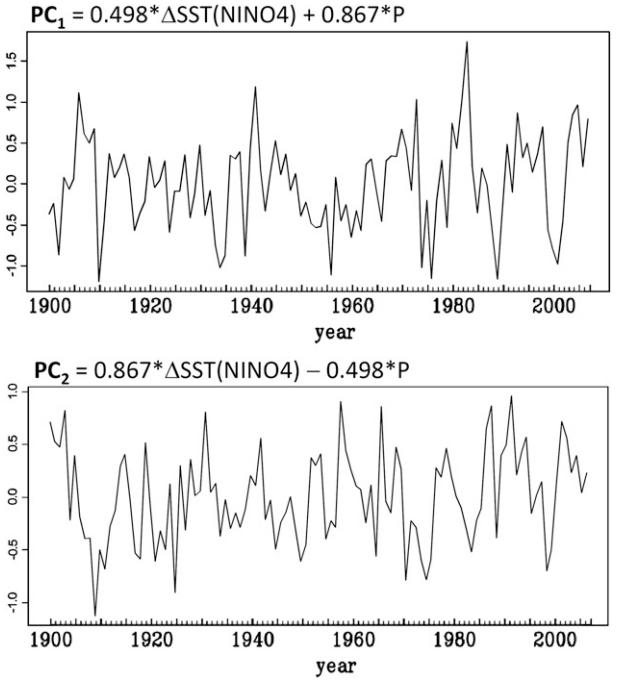

FIG. 3. Projection time series of (top) PC_1 and (bottom) PC_2 for the PCLag model.

The spectral coherence between ΔGSL and PC_1 (Fig. 2c) is strongest in the frequency band between 0.12 and 0.06, ~(9–17 yr), similar to the quasi-decadal variability that was found to coexist in ΔSST(NINO4), *P*, and the GSL elevation (Wang et al. 2010b). In addition, the coherence at the interannual frequency band (0.4) is stronger than that of *P*. A somewhat unexpected result is revealed in Fig. 2d: the coherence between ΔGSL and PC_2 is strong in the multidecadal frequency (<0.06). This feature echoes the recent finding by Wang and Gillies (2010, manuscript submitted to *J. Climate*) that the ΔGSL and local droughts both exhibit a marked, yet lagged, covariability with the interdecadal Pacific oscillation (IPO) (e.g., Zhang et al. 1997) within the 30–50-yr frequency band. These documented spectrums together are consistent with the leading spectral coherences between the GSL volume change and the Pacific climate variability (Mann et al. 1995). Hence, we constructed a lagged regression relating PC_1 and PC_2 to ΔGSL. Based on the same criteria as the PLag model, the best performing PCLag model was

$$\begin{aligned}\Delta\mathrm{GSL} = {} & 0.508\Delta\mathrm{GSL}(t-1) - 0.614\mathrm{PC}_1(t-8) \\ & - 0.416\mathrm{PC}_1(t-17) + 0.442\mathrm{PC}_1(t-42) \\ & + 0.722\mathrm{PC}_2(t-18),\end{aligned} \tag{3}$$

except at lag $t - 42$, all the coefficient betas in Eq. (3) exceeded the 0.05 significance level. The lag $t - 42$ here

and in the PLag model, as well as the lag $t - 18$, is also reflective of the ΔGSL's quarter-phase association with the IPO (Wang and Gillies 2010, manuscript submitted to *J. Climate*). As before, significant coefficient betas for shorter lags (<6 yr) were excluded, while the final lags chosen were comparable to those of the PLag model. For Eq. (3), the multiplied (adjusted) R^2 0.55 (0.51) and the autocorrelations of the residuals were insignificant. The P value of the Shapiro–Wilk normality test on the residual was 0.396. The RMSE between the fitted and observed ΔGSL was 0.859 feet, while the RMSE between the fitted and observed GSL elevation was 1.487 ft (Table 1).

As shown in Fig. 1b, the PCLag model (red line) successfully captured the characteristic quasi-decadal variability in ΔGSL, though certain aspects of the interannual variability were not captured; this is not unexpected as the bias is a compromise given our decision to omit short-term lags, and this likely resulted in the underestimation in the fitted ΔGSL around the peaks centered at 1984 and 1998. Although such a bias can be reduced by adding more lags for PC_1 between $t - 2$ and $t - 5$ (not shown), the added lags would increase the uncertainty of the forecast by at least a factor of 2. The reconstructed GSL elevation (Fig. 1c; red line) depicts the correct rhythm in the observed rises and declines but still inherits the bias of underestimated ΔGSL from 1983 onward. Nevertheless, the 8-yr forecast of the GSL elevation depicts a rising trend that intersects the observed elevation in 2009 and 2010[1]. According to the observations in Fig. 1a, the years around 2009 coincide with a warm-to-cold transition of ΔSST(NINO4) and a projected decline in the precipitation. Thus, the GSL elevation is expected to be in the process of integrating the increased precipitation around 2006 and should be on the rise. The PCLag model forecast is consistent with such a process.

A comparison of the RMSE′s for GSL elevation (Table 1) to first order would suggest that the PLag model is marginally better. To further compare the performance between the PLag and PCLag model, both models were used to make out-of-sample predictions. In regard to longer-term forecasting, predictions up to eight years ahead were made every year after 1985. All model coefficient betas were estimated exclusively on the in-sample dataset. The forecasting performance of the models was assessed on the out-of-sample dataset. Numerically, we have data X_t, t in years, and two predictors X^P (PLag) and X^{PC} (PCLag). These predictors depend on the final year t_f used for parameter estimation $X^P(t_f)$ and $X^{PC}(t_f)$, where $t_f < t$, and they were used to predict

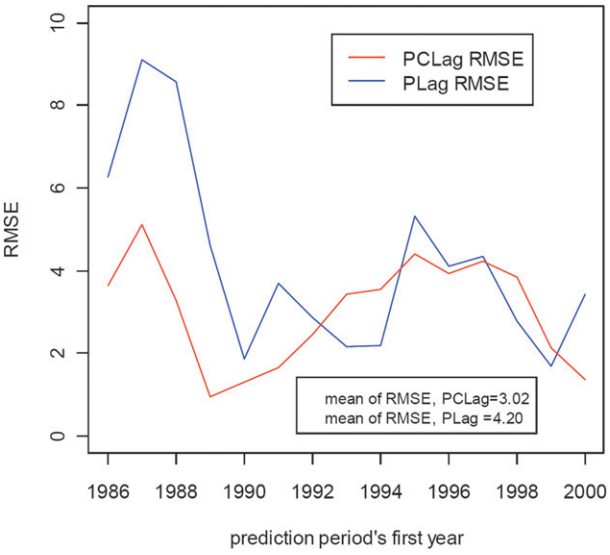

FIG. 4. The RMSEs of the PCLag model (red line) and the PLag model (blue line) for predictions up to eight years ahead made every year after 1985.

the next 8 years ahead. The out-of-sample prediction errors were then computed. The result is shown in Fig. 4. The RMSEs of the PCLag model are consistently smaller than those of the PLag model, except in four prediction periods starting 1992, 1993, 1997, and 1998. These years happened to be at the extreme phases of ENSO, which may distort or overpower the signal of the Pacific QDO (Wang et al. 2010a). The mean of the RMSEs of the PCLag model is 3.02—about one foot smaller than that of the PLag model, suggesting that the PCLag model performs better in predicting eight years ahead. It is also interesting to note that the PCLag model performs particularly well during the GSL "overturn" periods, such as in the periods of 1991–98 and 2000–07, when the GSL level bottomed out and began to rise (cf. Fig. 1c).

Three periods of the GSL elevation overturn time were further explored, which include 1) an upward trend turning downward (1986–93), 2) a downward trend turning upward (1991–98), and 3) the start of a downward trend (2000–07). During the period of 1986–93 (Fig. 5a), both the PLag and PCLag models predicted the GSL elevation to drop after the rising trend, but in each case the turning point is delayed by 2 yr. The PCLag model forecasted a continuous downward trend while the PLag model forecasted an upward trend after an initial downward trend, which disagreed with reality. For the period 1991–98 (Fig. 5b), both models forecasted the GSL elevation to rise after a few years of a downtrend trend, but the PCLag model aligned more closely with the observation. Finally for the 2000–07 period (Fig. 5c), the PLag model forecasted the 1999 peak but overestimated the 2004 trough, while the PCLag model underestimated the 1999

[1] The 2010 GSL elevation was measured up to 30 June; both the 2010 and 2009 data shown here are provisional.

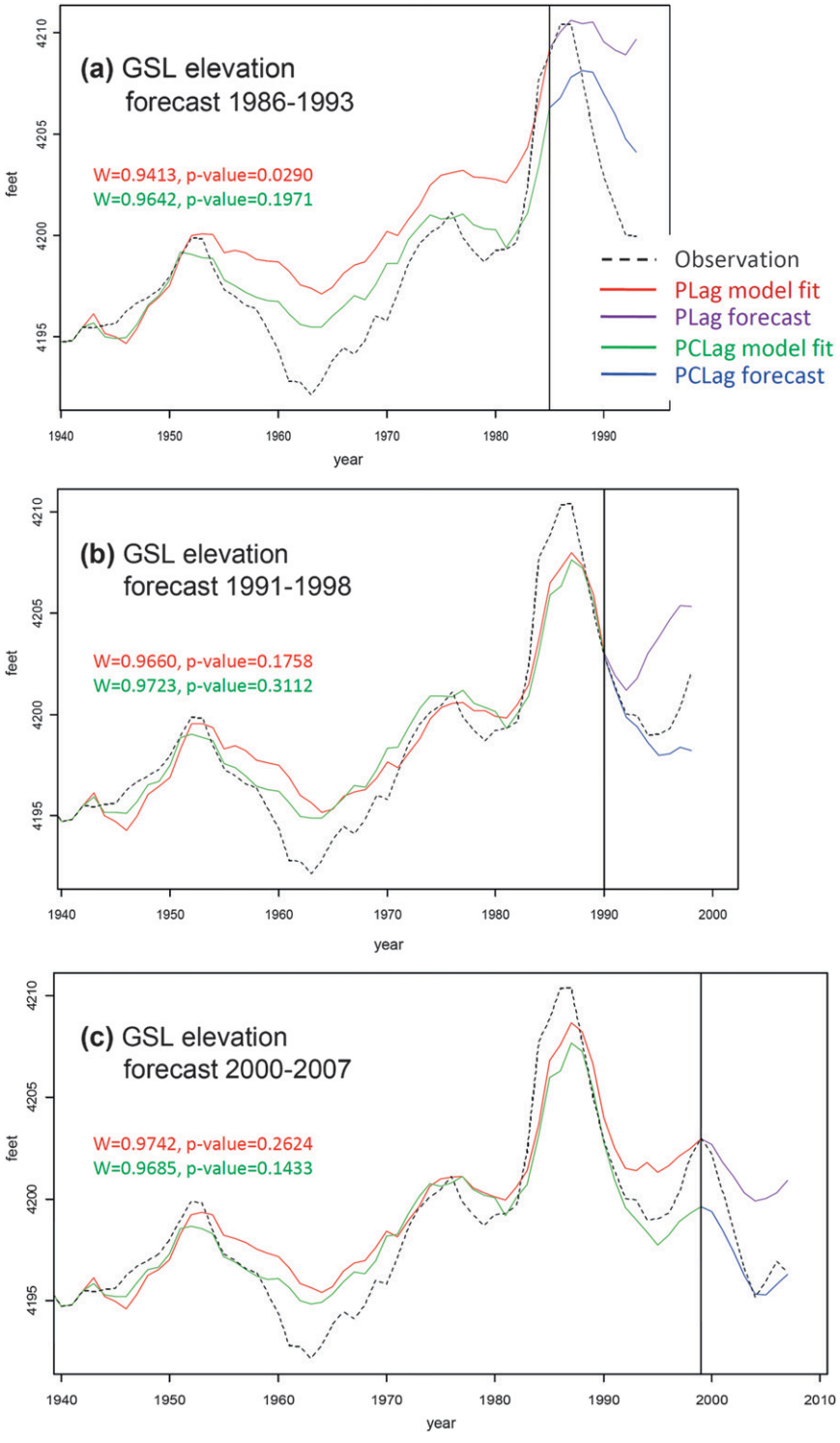

FIG. 5. The GSL elevation (black dashed curve) and model fits from the PLag model (red line) and the PCLag model (green line), along with the corresponding forecasts for the periods of (a) 1986–93, (b) 1991–98, and (c) 2000–07. Vertical lines indicate starting year of the forecast. The legend is provided alongside (a). The Shapiro–Wilk normality test results (W) for each model are provided.

TABLE 2. The RMSE between forecasts and observations.

	1986–93 (GSL downtrend)		1991–98 (GSL uptrend)		2000–07 (GSL downtrend)	
Period	ΔGSL (ft)	GSL (ft)	ΔGSL (ft)	GSL (ft)	ΔGSL (ft)	GSL (ft)
PLag model	1.552	6.258	1.108	3.693	0.945	3.416
SSTLag model	1.762	6.802	1.189	3.734	0.985	3.712
PCLag model	1.557	3.625	0.778	1.664	0.763	1.355

peak but captured the 2004 trough. The RMSEs of these forecasts are listed in Table 2.

4. Conclusions

A principal component analysis and a lagged regression model were combined to predict the ΔGSL and, subsequently, the GSL elevation. This approach is somewhat different from previous nonparametric, nonlinear time series forecasting for the GSL volume, since the ΔGSL has a strong hydrological linkage with local rainfall. Based on the lagged relationship between precipitation in the GSL watershed and the Pacific QDO observed previously, we used the annual means of P and the water year means of ΔSST(NINO4) as the predictor variables transformed with PC analysis. The results show that the PCLag model was able to forecast the characteristic turnarounds of the GSL elevation, in which a prolonged increasing trend is followed by a persistent decrease or vice versa. Although previous short-term forecasts were able to predict the GSL volume out to four years in advance during extreme hydrologic events, those short-term forecasts were generally unable to capture the turnarounds of the GSL volume (e.g., Fig. 6 of Lall et al. 2006; Fig. 6 of Moon et al. 2008). Thus, the ability of the PCLag model to estimate the GSL elevation turnarounds is a noteworthy improvement. However, forecasts of the PCLag model exhibit biases in the GSL elevation due in part to the lack of shorter-term (interannual) variability—a trade-off given a desire for longer-term forecast capability. One remedy to this situation might be to couple the proposed longer-term forecast with the established short-term forecast methods.

Acknowledgments. We are indebted to David Stoffer for providing useful *R*-code that facilitated our statistical analyses. This study was supported by the USDA CSREES–funded Drought Management, Utah Project, and approved as journal number 8230 by the Utah Agricultural Experiment Station, Utah State University.

REFERENCES

Abarbanel, H. D. I., and U. Lall, 1996: Nonlinear dynamics of the Great Salt Lake: System identification and prediction. *Climate Dyn.,* **12,** 287–297.

James, D., D. S. Bowles, R. V. Canfield, D. G. Chadwick, N. Stauffer, and P. J. Riley, 1984: Estimating water surface elevation probabilities for the Great Salt Lake. Utah Water Research Laboratory Rep., 37 pp.

Kaplan, A., M. A. Cane, Y. Kushnir, A. C. Clement, M. B. Blumenthal, and B. Rajagopalan, 1998: Analyses of global sea surface temperature 1856–1991. *J. Geophys. Res.,* **103,** 18 567–18 589.

Lall, U., and M. E. Mann, 1995: The Great Salt Lake: A barometer of low-frequency climatic variability. *Water Resour. Res.,* **31,** 2503–2515.

——, T. Sangoyomi, and H. Abarbanel, 1996: Nonlinear dynamics of the Great Salt Lake: Nonparametric short-term forecasting. *Water Resour. Res.,* **32,** 975–985.

——, Y.-I. Moon, H.-H. Kwon, and K. Bosworth, 2006: Locally weighted polynomial regression: Parameter choice and application to forecasts of the Great Salt Lake. *Water Resour. Res.,* **42,** 1–11.

Mann, M., U. Lall, and B. Saltzman, 1995: Decadal-to-centennial-scale climate variability: Insights into the rise and fall of the Great Salt Lake. *Geophys. Res. Lett.,* **22,** 937–940.

Meehl, G. A., J. M. Arblaster, K. Matthes, F. Sassi, and H. van Loon, 2009: Amplifying the Pacific climate system response to a small 11-year solar cycle forcing. *Science,* **325,** 1114–1118.

Moon, Y.-I., and U. Lall, 1996: Atmospheric flow indices and interannual Great Salt Lake variability. *J. Hydrol. Eng.,* **1,** 55–62.

——, ——, and H.-H. Kwon, 2008: Non-parametric short-term forecasts of the Great Salt Lake using atmospheric indices. *Int. J. Climatol.,* **28,** 361–370.

Sangoyomi, T., U. Lall, and H. Abarbanel, 1996: Nonlinear dynamics of the Great Salt Lake: Dimension estimation. *Water Resour. Res.,* **32,** 149–159.

Shanahan, T. M., J. T. Overpeck, W. E. Sharp, C. A. Scholz, and J. A. Arko, 2007: Simulating the response of a closed-basin lake to recent climate changes in tropical West Africa (Lake Bosumtwi, Ghana). *Hydrol. Processes,* **21,** 1678–1691.

Shumway, R. H., and D. S. Stoffer, 2006: *Time Series Analysis and Its Applications: With R Examples*. 2nd ed. Springer, 569 pp.

Wang, S.-Y., R. R. Gillies, L. E. Hipps, and J. Jin, 2010a: A transition-phase teleconnection of the Pacific quasi-decadal oscillation. *Climate Dyn.,* **36,** 681–693, doi:10.1007/s00382-009-0722-5.

——, ——, J. Jin, and L. E. Hipps, 2010b: Coherence between the Great Salt Lake level and the Pacific quasi-decadal oscillation. *J. Climate,* **23,** 2161–2177.

White, W. B., and Z. Liu, 2008: Resonant excitation of the quasi-decadal oscillation by the 11-year signal in the sun's irradiance. *J. Geophys. Res.,* **113,** C01002, doi:10.1029/2006JC004057.

Zhang, Y., J. M. Wallace, and D. S. Battisti, 1997: ENSO-like interdecadal variability: 1900–93. *J. Climate,* **10,** 1004–1020.